Histol Histopathol (2022) 37: 35-42

http://www.hh.um.es

Histology and Histopathology
From Cell Biology to Tissue Engineering

ORIGINAL ARTICLE **Open Access**

Protruding structures with high expression of LGR5 are formed during regrowth phase after chemo-treatment in xenograft model of colorectal adenocarcinoma

Masaki Yamazaki[1], Atsuhiko Kato[1], Noriaki Sawada[1], Takeshi Watanabe[2] and Masami Suzuki[1]

[1]Research Division, Chugai Pharmaceutical Co. Ltd., Kajiwara, Kamakura, Kanagawa and

[2]Chugai Research Institute for Medical Science, Inc., Komakado, Gotemba, Shizuoka, Japan

Summary. Recurrence after chemotherapy is one of the biggest obstacles in cancer therapy, along with metastasis. Although histopathological evaluation in preclinical models like the xenograft model help us to understand the pathophysiological process of tumor growth, there are not enough detailed histopathological analyses of such models. In this study, to learn how a tumor recovers the typical tumor structure after structural corruption during chemo-treatment, xenografted tumors originating from a patient-derived xenograft of colorectal cancer (CRC) were analyzed histopathologically over time. There were many Duct (Flattened) at Day 1 (one day after the final administration of Irinotecan), but the ratio of Duct (Columnar) and Cribriform—structures typically found in colorectal adenocarcinoma—increased over time. Finally, at Day 15 (15 days after the final administration of Irinotecan), tumor structure and size were once again the same as in the control group. LGR5, a known cancer stem cell (CSC) marker for CRC, was highly expressed on protruding structures observed from Duct (Flattened) during their transformation into Duct (Columnar) and Cribriform. In addition, these LGR5-expressing protruding structures were either Ki67 negative or positive. These results suggest that the formation of protruding structures on Duct (Flattened) is a pivotal first step in the regrowth of tumors.

Key words: LGR5, Protruding structure, Duct (Flattened), After chemo-treatment, Colorectal cancer

Corresponding Author: Masaki Yamazaki, DVM, Research Division, Chugai Pharmaceutical Co., Ltd., 200, Kajiwara, Kamakura, Kanagawa 247–8530, Japan. e-mail: yamazakimsk@chugai-pharm.co.jp

DOI: 10.14670/HH-18-374

Introduction

Recurrence after chemotherapy is one of the biggest obstacles in cancer therapy, along with metastasis. Although mortality associated with colorectal cancer (CRC) diagnosis has declined progressively in recent decades because of improved surgical techniques and the availability of more effective systemic therapies (Dienstmann et al., 2017), CRC unfortunately still returns in 30 to 40% of patients following treatment originally hoped to cure the disease (Duineveld et al., 2016).

The morphological features of residual tumor cells have been well reported for rectal cancer after chemoradiotherapy and CRC with hepatic metastasis after chemotherapy (Pai and Pai, 2018). Take for example, fibrous/fibroinflammatory tissue, hemosiderin-laden foamy macrophages, colloid response mucin lakes, eosinophilic cytoplasm, oncocytic differentiation, elongated stratified basophilic cells, nuclear hyperchromasia, atypia, neuroendocrine differentiation, cytoplasmic vacuolization, prominent nucleoli, and cystic dilatation (Shia et al., 2004; O'Neil and Damjanov, 2009; Hav et al., 2015; Pai and Pai, 2018). However, there are few detailed preclinical reports that have qualitatively evaluated residual tumor cells after chemo-treatment (Brown et al., 2018), even though preclinical models could potentially reveal the mechanism of recurrence. Preclinical models allow us to observe the cells over time, giving us access to a pathophysiological process not seen with clinical samples.

Cancer stem cells (CSC) are known to survive chemotherapy as a residual subpopulation and the source of recurrence (Batlle and Clevers, 2017; Shibue and Weinberg, 2017). In our previous study using a patient-derived xenograft model (PDX), the expression of LGR5, a marker for CSC (Barker et al., 2009; Shimokawa et al., 2017), was suppressed during irinotecan treatment, but recovered when the treatment was withdrawn, leading to the reformation of typical

tumor structure (Kobayashi et al., 2012). However, we have yet to investigate the relationship between re-expression of LGR5 and specific morphological features. This could give us a deeper understanding of the mechanism of recurrence.

In this study, to discover how tumors recover their typical structure during regrowth after chemo-treatment, we elucidated the transition between morphological features and their relationship with LGR5 expression using a xenograft model with a PDX-derived CRC cell line.

Materials and methods

Cell line

A stable human CRC cell line expressing LGR5 and possessing CSC properties (PLR123) was cultured as previously described (Kobayashi et al., 2012). The LGR5-positive CSC line (PLR123) was established from a CRC PDX model after serial passages in NOD/Shi-scid IL-2RγKO (NOG) mice and the subsequent adherent cell culture of tumors. The PLR123 cell line was derived from moderately differentiated colon cancer, and the microsatellite status was confirmed by immunohistochemistry for MLH-1 (negative), MSH2 (positive), MSH6 (positive) and PMS2 (negative) in this study (data not shown).

Irinotecan treatment study using LGR5-positive CSC bearing NOG mice

18 NOG mice (CLEA Japan) were divided into six groups. 12 days after inoculation with LGR5-positive CSC ($1x10^5$, sc) (Day -6), NOG mice were administered irinotecan (120 mg/kg, ip, Yakulto Honsha, Japan) three times with 2 day intervals (Kobayashi et al., 2012). Xenotransplanted tumor tissues were removed from each animal after sacrifice by exsanguination under isoflurane anesthesia on Day 1, 3, 6, 9, and 15 (after the final administration) (n=3) for pathological evaluation. One group was assigned as control group (n=3), and were sacrificed at Day 3 (21 days after inoculation) without any treatment. The tumor reached the appropriate size (approx. 300 mm^3) for pathological observation on Day 3. Tumor volume was measured on the day of sacrifice. All animal experiments were approved by the Ethical Committee for Treatment of Laboratory Animals at Chugai Pharmaceutical Co., Ltd.

Tissue preparation

Xenograft samples were divided along the largest cross-section, and fixed with 4% paraformaldehyde (PFA) at 4°C for 16-24 hr. All samples were processed and embedded in paraffin by the AMeX method (Suzuki et al., 2000), and hematoxylin and eosin (HE)-stained sections were produced by the standard method.

Histopathological evaluation

To evaluate tumor morphology, certified D.V.M. pathologists (MS and MY) defined four types of structures: Duct (Columnar), having a single layer of columnar tumor cells; Cribriform, having multiple layers of columnar tumor cells with ambiguous duct to duct interaction (the lumens were counted); Cluster, a cluster of tumor cells without a ductal structure; and Duct (Flattened), having flat tumor cells. Because of a range in the ratios of flat to columnar cells in Duct (Flattened), the Ductal (Flattened) was defined as having a flattened area greater than one-third of the whole circumference. Over 100 structures located from the interface to the center of the tumor mass were counted. Then, the ratio for the four types of structures was calculated.

Detection of LGR5 on sectioned slides

It is well known that a very low level of LGR5 protein is expressed in tissues. Therefore, the tyramide method was performed to detect LGR5 as previously described (Kobayashi et al., 2012; Yamazaki et al., 2015, 2021). Sectioned specimens from the above-mentioned paraffin blocks were incubated with LGR5 antibody (2U2E-2, in-house). After incubation with the primary antibody, the sections were incubated with a secondary antibody conjugated with polymer-horseradish peroxidase (HRP) (DAKO, CA, USA) and the reaction was visualized by Alexa Fluor 488-labeled tyramide (Life Technologies).

Immunofluorescence

Sectioned specimens from the above-mentioned paraffin blocks were incubated with anti-HLA-DMA antibody (Sigma-Aldrich, MO, USA) and anti-Ki67 antibody (Abcam, Cambridge, UK). After incubation with the primary antibodies, sections were incubated with a secondary antibody conjugated with biotin (Vector Laboratories, CA, USA) and the proteins were visualized by Alexa Fluor 568-labeled streptavidin (Life technologies). Those specimens were also stained with DAPI. Observation were conducted by confocal microscope (C1, Nikon, Tokyo, Japan).

Quantification of LGR5-positive area

The LGR5-positive area in tumor was calculated using the 'Area Quantification FL v2.1.6' algorithm within the HALO AI image analysis software (Indica Labs, NM, USA, v3.2). Tumor areas in each observation site were manually annotated and evaluated by a pathologist (MY). The LGR5-positive area was expressed in the tumor area of the observation area (%).

Immunohistochemistry

Immunohistochemical staining with primary

antibodies to MLH-1 (M1, Roche Diagnostics, IN, USA), MSH2 (G219-1129, Roche Diagnostics), MSH6 (SP93, Roche Diagnostics) and PMS2 (A16-4, Roche Diagnostics) was performed with Ventana BenchMark XT automated stainer (Roche Diagnostics) according to the maker's recommendation. Briefly, the sectioned tissues were deparaffinized, heat pretreated in Cell Conditioning 1 (CC1) for antigen retrieval in 95-100°C for 40-92 min, and then incubated with the primary antibodies for 12-32 min at 37°C. Amplification was performed by the OptiView Amplification kit (Roche Diagnostics) for PMS2. The slides were incubated with a secondary antibody followed by the application of HRP Universal Multimer (Roche Diagnostics). Antibodies were detected using DAB and slides were counterstained with hematoxylin II (Roche Diagnostics).

Results

Tumor volume

The tumor (PLR123) bearing mice were administered a maximum tolerated dose (120 mg/kg) of irinotecan 3 times (Fig. 1A). The tumor volume in the treatment group was lower than in the control group from Day 1 to 6, but at Day 9 and 15 the tumor volume was again the same (Fig. 1B).

Duct (Flattened) formed after chemotherapy was replaced by Duct (Columnar) and cribriform duct over time

Instead of the typical ductal structure composed of columnar cells seen in the control group, Duct (Flattened) were mainly found in the center of the tumor from Day 1, but the typical structure was almost recovered at Day 9 or 15 according to low magnification images (Fig. 2A). As described in Materials and Methods, four types of structure were identified within tumors; Duct (Columnar), Cribriform, Clusters, and Duct (Flattened) were observed in the control or treatment groups (Fig. 2B, C). There was a range in the ratio of the flattened area to the Duct (Flattened) (Fig. 2C). The flattened area covers almost the whole circumference of the Duct (Flattened) in the upper image in Fig. 2C, but in the lower image the flattened area is only one-third the circumference with the rest already transformed into columnar cells. The transition in ratio for these structures is shown in Fig. 2D. As in the low magnification images, the main component at Day 1 was the Duct (Flattened), which was not observed in the control group. Gradually, the Duct (Flattened) were replaced by Duct (Columnar) until, finally, on Day 15, the ratio was almost the same as in the control group, although a small number of Duct (Flattened) remained.

LGR5 is highly expressed in the protruding structure of Duct (Flattened) after chemo-treatment.

At Day 1, the expression of LGR5 was barely observed in the center of the tumor (Fig. 3A). At Day 6, LGR5-positive cells appeared in the center of the tumor as clusters (Fig. 3A, white arrowheads). The quantitative analysis of LGR5-positive area including the interface to the center of the tumor is shown in Fig. 3B. The ratio of LGR5-positive area was low on Day 1, increased on Day 3 and 6, and decreased from Day 6 to Day 9. At Day 1, HLA-DMA, a stem cell marker for non-proliferating cells (Kobayashi et al., 2012), was expressed in Duct (Flattened) as seen at high magnification (Fig. 3C). At Day 6, LGR5-positive cells were predominantly located in protruding structures alongside the Duct (Flattened) (Fig. 3D). The protruding structures included high columnar cells which sometimes aligned in a fan-like shape with the lumen (Fig. 3E). This composition was confirmed using a 3D structure reconstructed from semi-serial sections (Fig. 3F). Furthermore, protruding structures highly expressing LGR5 were either Ki67-negative or -positive (Fig. 4).

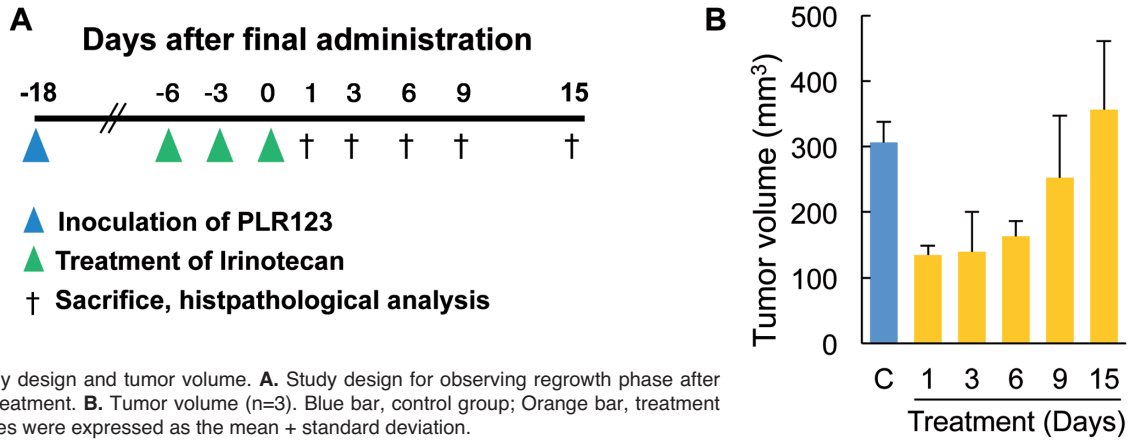

Fig. 1. Study design and tumor volume. **A.** Study design for observing regrowth phase after irinotecan treatment. **B.** Tumor volume (n=3). Blue bar, control group; Orange bar, treatment group. Values were expressed as the mean + standard deviation.

LGR5 expresses in protruding structure after chemo-treatment

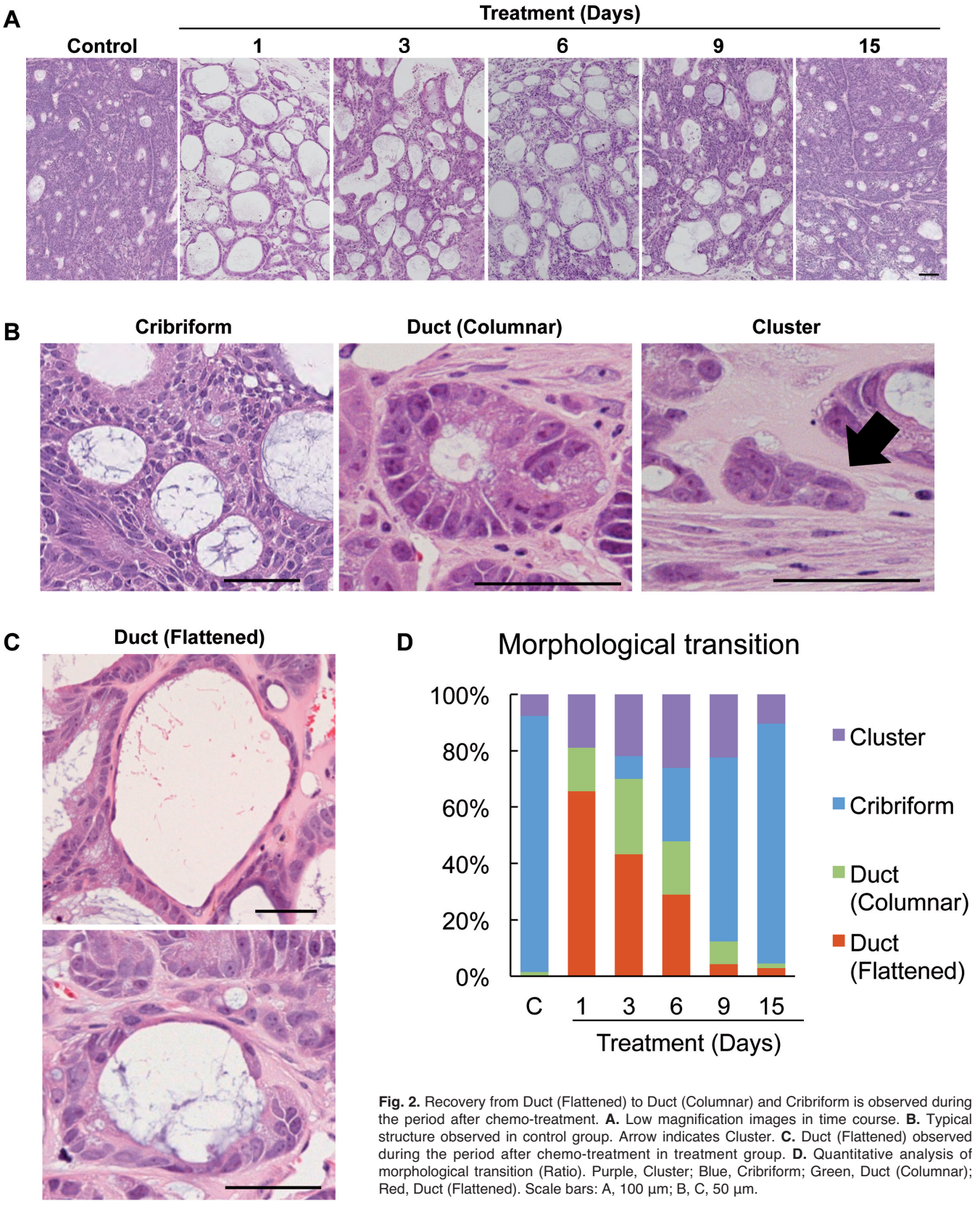

Fig. 2. Recovery from Duct (Flattened) to Duct (Columnar) and Cribriform is observed during the period after chemo-treatment. **A.** Low magnification images in time course. **B.** Typical structure observed in control group. Arrow indicates Cluster. **C.** Duct (Flattened) observed during the period after chemo-treatment in treatment group. **D.** Quantitative analysis of morphological transition (Ratio). Purple, Cluster; Blue, Cribriform; Green, Duct (Columnar); Red, Duct (Flattened). Scale bars: A, 100 μm; B, C, 50 μm.

Discussion

In this study we evaluated morphological changes and their relationship to the expression of LGR5 during tumor regrowth after chemo-treatment using a xenograft model with a PDX-derived CRC cell line. This is just one example of the regrowth process, and it uses a cell line that we already know expresses LGR5. To fully understand regrowth after chemotherapy, further investigation is needed. A schematic detailing the process of regrowth after chemotherapy is shown in Fig. 5.

The Duct (Flattened) is a unique morphological feature that emerges after chemo-treatment. A previous report revealed flat or rounded nuclei oriented in the basal side of cells in a PDX model of CRC following treatment with irinotecan plus 5-FU (Brown et al., 2018). This coincides with cystic dilatation observed in resected clinical specimens from CRC after neoadjuvant

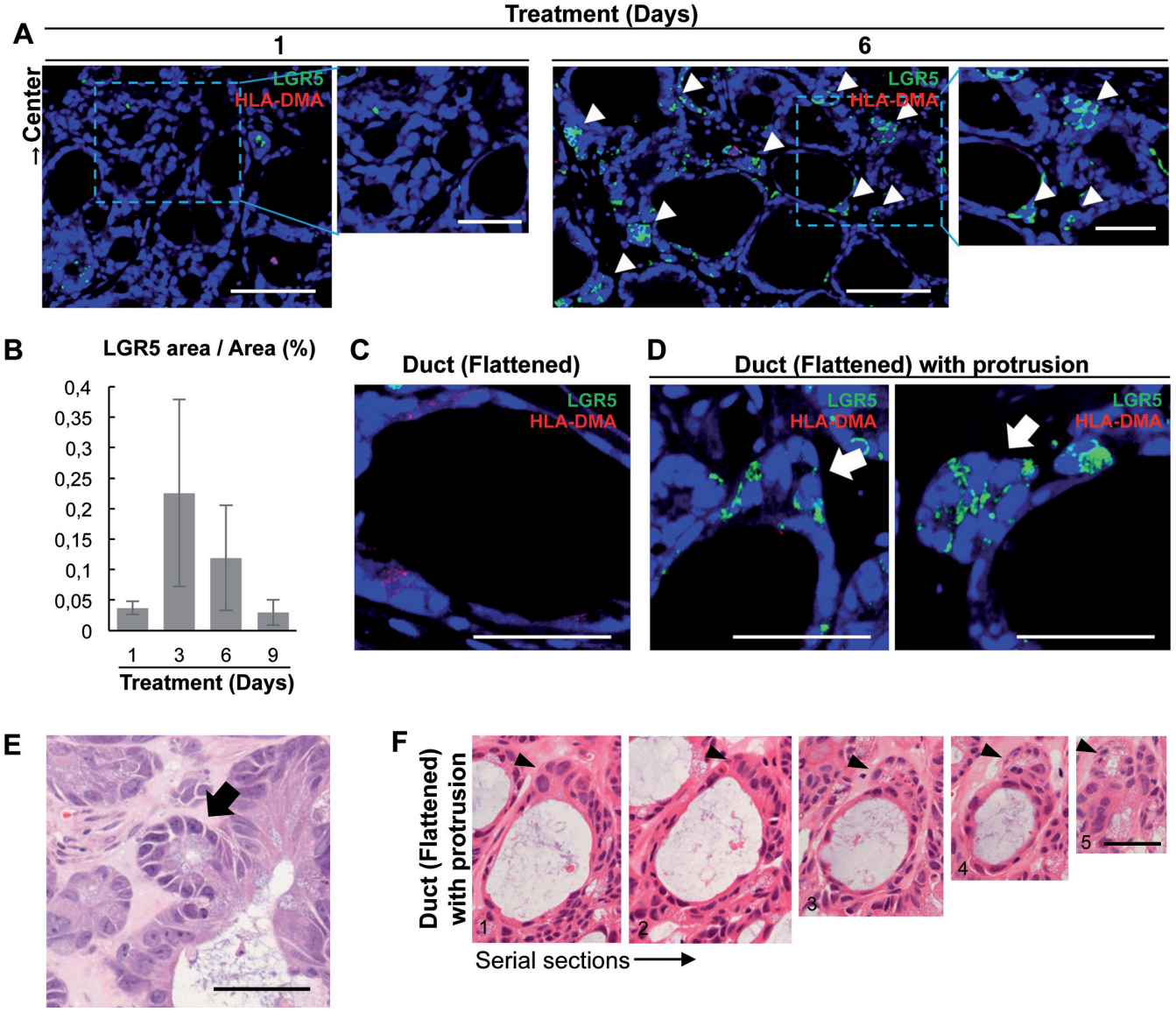

Fig. 3. Protruding structure in Duct (Flattened) expresses LGR5 highly during the period after chemo-treatment. **A.** Distribution of LGR5 (green) and HLA-DMA (red) positive cells in a low magnification image at Day 1 and 6. White arrowheads indicate protruding structures with LGR5-positive cells. Multiple photos were combined into one image. **B.** Quantitative analysis for LGR5-positive area. Values were expressed as the mean ± standard deviation. High magnification images of Duct (Flattened) **C.** and Duct (Flattened) with protruding structure **D.** LGR5 (green), HLA-DMA (red). Arrows indicate protruding structures. **E.** An image for protruding structure in HE. Arrow indicates protruding structure. **F.** Serial section images of Duct (Flattened) with protruding structure. Numbers in pictures show the order of semi-serial sections. Arrowheads indicate protruding structures. Scale bars: A, 100 μm for low magnification (left) and 50 μm for high magnification (right), C-F, 50 μm.

therapy (O'Neil and Damjanov, 2009). Many of the cells composing ducts were eliminated by chemo-treatment, with residual cells elongating to preserve the tissue structure (Dekoninck and Blanpain, 2019). This is why the duct has a cystic shape. A crucial factor in the formation of the cystic duct is the preservation of surrounding stroma and basement membrane. Preservation of the scaffold minimizes changes to tissue structure. With stronger chemo-treatment, the stroma including the basement membrane is destroyed, which may lead to the greater collapse of tissue structure (Mancini and Sonis, 2014).

As a typical tumor structure re-emerges from Duct (Flattened), we discover an interesting morphological feature: flat cells composing a duct transformed from cuboidal cells, forming a unique protruding structure which highly expresses LGR5, a CSC marker (Barker et al., 2009; Shimokawa et al., 2017). Thus, this LGR5-expressing protruding structure works as a starting point for recurrence. Either the typical ductal structure recovers along the original basement membrane, or the protruding structure—which sometimes already has a lumen of its own—forms new a ductal structure. Even in cases of standard tumor growth without chemo-treatment, continuous formation of small clusters composed of high LGR5-expressing tumor cells have been reported in the invasive front in a CRC xenograft model (Yamazaki et al., 2021). Thus, LGR5-positive tumor cell clusters are considered to be an important structural starting point for CRC tumor growth with or without chemo-treatment.

The protruding structure is characterized molecularly by strong LGR5 positive expression accompanied with either Ki67-negative or -positive

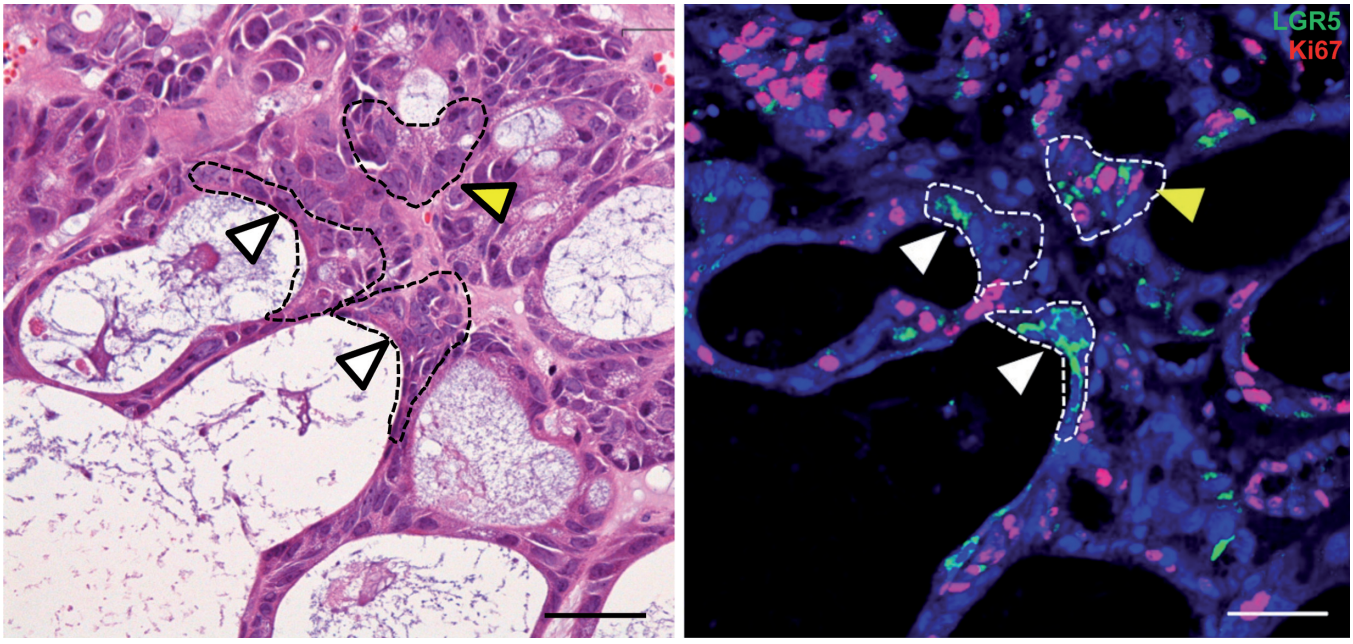

Fig. 4. Proliferation states in protruding structure. Images show expression of LGR5 (green) and Ki67 (red) in protruding structures. Protruding structures are enclosed by dotted line. White arrowheads indicate LGR5+/Ki67- and a yellow arrowhead indicates LGR5+/Ki67+ protruding structures. Scale bars: 50 μm.

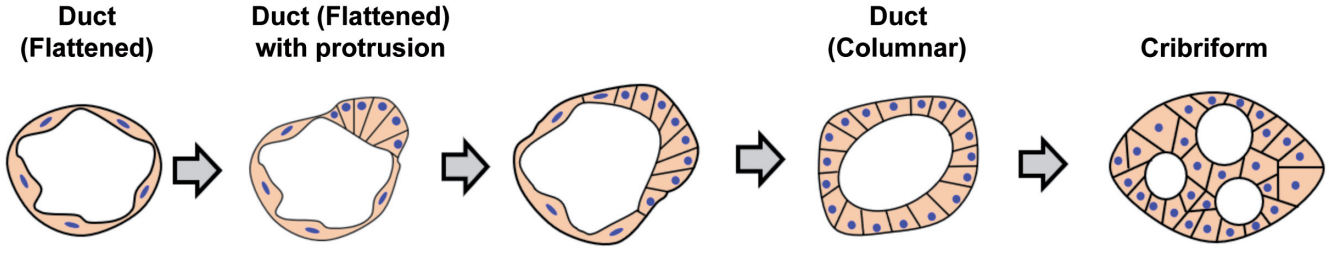

Fig. 5. Schematic of protruding structure in regrowth phase after chemo-treatment.

expression. In Duct (Flattened), LGR5 expression was almost non-existent, and HLA-DMA, a dormant CSC marker (Kobayashi et al., 2012), was expressed instead. Stem cell properties are preserved during the interconversion between LGR5- and HLA-DMA-positive cells (Kobayashi et al., 2012). In our previous study, we concluded that LGR5-positive cells proliferate and HLA-DMA-positive cells remain dormant based on immunohistochemistry results showing a correlation between LGR5- and Ki67-positive, and HLA-DMA-positive and Ki67-negative (Kobayashi et al., 2012). However, in the current study we confirmed that LGR5-positive cells show both Ki67-negative and -positive expression in the protruding structure of Duct (Flattened). It is assumed that LGR5-positive cells exist in a range from non-proliferating to proliferating. In fact, heterogeneity has been reported within the Lgr5+ intestinal stem cell pool in a mouse model, and slowly cycling subpopulations of Lgr5+ were shown to contribute to all intestinal lineages (Barriga et al., 2017). Interestingly, the slow-cycling Lgr5+ population is spared by chemotherapy, surviving to assist in regenerating the normal intestinal epithelium following toxic insults. Basically, chemotherapy kills the cycling cells, but not the slow cells, leaving the slow cells to replenish the cycling cells. This phenomenon is similar to that observed during tumor regrowth after chemo-treatment in our study.

In conclusion, we elucidated how LGR5-positive protruding structures in Duct (Flattened) act as a starting point in the reformation of a typical tumor structure after chemo-treatment in a xenograft model using a PDX-derived CRC cell line. This unique protruding structure can be the focus of CSC therapy that goes beyond simply targeting LGR5-positive cells, by also striking at the molecular mechanisms that initiate the recurrence of tumors after chemo-therapy. We believe this knowledge will broaden the possibilities of CSC therapy after chemotherapy in the future.

Acknowledgements. We thank Yayoi Takai (Chugai Research Institute for Medical Science, Inc.) and Naoko Awasaki (Chugai Pharmaceutical Co., Ltd.) for help with pathological techniques. We are also grateful to Dr. Tatsumi Yamazaki (Chugai Pharmaceutical Co., Ltd.) for his encouragement.

Conflicts of Interest. M.Y., A.K., N.S., and M.S. are employees of Chugai Pharmaceutical Co., Ltd. T.W. is an employee of Chugai Research Institute for Medical Science, Inc.

References

Barker N., Ridgway R.A., Van Es J.H., Van De Wetering M., Begthel H., Van Den Born M., Danenberg E., Clarke A.R., Sansom O.J. and Clevers H. (2009). Crypt stem cells as the cells-of-origin of intestinal cancer. Nature 457, 608-611.

Barriga F.M., Montagni E., Mana M., Mendez-Lago M., Hernando-Momblona X., Sevillano M., Guillaumet-Adkins A., Rodriguez-Esteban G., Buczacki S.J.A., Gut M., Heyn H., Winton D.J., Yilmaz O.H., Attolini C.S.O., Gut I. and Batlle E. (2017). Mex3a marks a slowly dividing subpopulation of lgr5+ intestinal stem cells. Cell Stem Cell 20, 801-816.

Batlle E. and Clevers H. (2017). Cancer stem cells revisited. Nat. Med. 23, 1124-1134.

Brown K.M., Xue A., Julovi S.M., Gill A.J., Pavlakis N., Samra J.S., Smith R.C. and Hugh T.J. (2018). Using patient-derived xenograft models of colorectal liver metastases to predict chemosensitivity. J. Surg. Res. 227, 158-167.

Dekoninck S. and Blanpain C. (2019). Stem cell dynamics, migration and plasticity during wound healing. Nat. Cell Biol. 21, 18-24.

Dienstmann R., Vermeulen L., Guinney J., Kopetz S., Tejpar S. and Tabernero J. (2017). Consensus molecular subtypes and the evolution of precision medicine in colorectal cancer. Nat. Rev. Cancer 17, 79-92.

Duineveld L.A.M., van Asselt K.M., Bemelman W.A., Smits A.B., Tanis P.J., van Weert H.C.P.M. and Wind J. (2016). Symptomatic and asymptomatic colon cancer recurrence: A multicenter cohort study. Ann. Fam. Med. 14, 215-220.

Hav M., Libbrecht L., Ferdinande L., Geboes K., Pattyn P. and Cuvelier C.A. (2015). Pathologic assessment of rectal carcinoma after neoadjuvant radio(chemo)therapy: Prognostic implications. Biomed. Res. Int. 574540.

Kobayashi S., Yamada-Okabe H., Suzuki M., Natori O., Kato A., Matsubara K., Jau Chen Y., Yamazaki M., Funahashi S., Yoshida K., Hashimoto E., Watanabe Y., Mutoh H., Ashihara M., Kato C., Watanabe T., Yoshikubo T., Tamaoki N., Ochiya T., Kuroda M., Levine A.J. and Yamazaki T. (2012). LGR5-positive colon cancer stem cells interconvert with drug-resistant LGR5-negative cells and are capable of tumor reconstitution. Stem Cells 30, 2631-2644.

Mancini M.L. and Sonis S.T. (2014). Mechanisms of cellular fibrosis associated with cancer regimen-related toxicities. Front. Pharmacol. 27, 51.

O'Neil M. and Damjanov I. (2009). Histopathology of colorectal cancer after neoadjuvant chemoradiation therapy. Pathol. J. 3, 91-98.

Pai R.K. and Pai R.K. (2018). Pathologic assessment of gastrointestinal tract and pancreatic carcinoma after neoadjuvant therapy. Mod. Pathol. 31, 4-23.

Shia J., Guillem J.G., Moore H.G., Tickoo S.K., Qin J., Ruo L., Suriawinata A., Paty P.B., Minsky B.D., Weiser M.R., Temple L.K., Wong W.D. and Klimstra D.S. (2004). Patterns of morphologic alteration in residual rectal carcinoma following preoperative chemoradiation and their association with long-term outcome. Am. J. Surg. Pathol. 28, 215-223.

Shibue T. and Weinberg R.A. (2017). EMT, CSCs, and drug resistance: the mechanistic link and clinical implications. Nat. Rev. Clin. Oncol. 14, 611-629.

Shimokawa M., Ohta Y., Nishikori S., Matano M., Takano A., Fujii M., Date S., Sugimoto S., Kanai T. and Sato T. (2017). Visualization and targeting of lgr5+ human colon cancer stem cells. Nature 545, 187-192.

Suzuki M., Adachi K., Ogawa Y., Karasawa Y., Katsuyama K., Sugimoto T. and Doi K. (2000). The combination of fixation using PLP fixative and embedding in paraffin by the AMeX method is useful for immunohistochemical and enzyme histochemical studies of the lung. J. Toxicol. Pathol. 13, 109-113.

Yamazaki M., Kato A., Zaitsu Y., Watanabe T., Iimori M., Funahashi S., Kitao H., Saeki H., Oki E. and Suzuki M. (2015). Intensive

immunofluorescence staining methods for low expression protein: Detection of intestinal stem cell marker LGR5. Acta Histochem. Cytochem. 48, 159-164.

Yamazaki M., Kato A., Oki E., Zaitsu Y., Kato C., Nakano K., Nakamura M., Sakomura T., Kawai S., Fujii E., Sawada N., Watanabe T., Saeki H. and Suzuki M. (2021). Continuous formation of small clusters with LGR5-positive cells contributes to tumor growth in a colorectal cancer xenograft model. Lab. Invest. 101, 12-25.

Accepted September 8, 2021